Journal of Colloid and Interface Science **244,** 190–199 (2001)
doi:10.1006/jcis.2001.7868, available online at http://www.idealibrary.com on IDEAL®

# The Influence of Charge Variation on the Adsorbed Configuration of a Model Cationic Oligomer onto Colloidal Silica

YongWoo Shin,* James E. Roberts,† and Maria Santore*,[1,2]

*Department of Chemical Engineering and †Department of Chemistry, Lehigh University, Bethlehem, Pennsylvania 18015

Received April 27, 2001; accepted July 21, 2001; published online October 24, 2001

**The adsorbed amounts and interfacial conformations of a low-molecular-weight oligomer of a weak cationic polyelectrolyte (15-unit chain of dimethylaminoethyl methacrylate, DMAEMA) on colloidal silica were examined, with the ultimate intent of providing perspective on the adsorption of high-molecular-weight weak polyelectrolytes. At all but the lowest ionic strengths or highest pHs, over the full range of adsorbed oligomer amounts on each isotherm, the interfacial conformation was relatively insensitive to coverage with train fractions from 0.8 to 1. This occurs because short oligomeric chains are not capable of forming long loops or tails found in higher-molecular-weight homopolymer layers. Variations in pH altered the backbone and surface charge densities, changing the density of contact points for adsorption. This was apparent in the NMR solvent relaxation behavior, which suggested the tightest binding near pH 6, and a sharp drop in the train fraction at high pH, just as the adsorption began to diminish with reduced backbone protonation. Variations in ionic strength screened repulsions among adsorbed oligomers, an effect most apparent at low ionic strengths. NMR solvent relaxation data provided substantial evidence for differences in the anchoring of DMAEMA oligomer and adsorbed trains of a nonionic homopolymer such as polyethylene oxide (T. Cosgrove, M. A. Cohen Stuart, and G. P. van der Beek,** *Langmuir* **7, 327 (1991)). DMAEMA adsorbs at a small number of discrete points on side chains, while with polyethylene oxide the literature suggested every monomer on the main backbone can potentially adhere to the surface, giving a less mobile interface from the perspective of the solvent.** 

*Key Words:* **polyelectrolyte oligomer adsorption; weak polyelectrolyte; train fraction; bound fraction.**

## INTRODUCTION

Polyelectrolytes play important roles in colloidal dispersions: As high-molecular-weight polymers, they act as flocculants for wastewater treatment and papermaking. Low-molecular-weight polycation blocks in copolymer systems may serve as anchoring groups on stabilizers, or as the stabilizing block, depending on the relative surface affinity for the two polymer components. These systems are therefore of interest from a practical perspective, but the complex physics of adsorbing polyelectrolytes are only recently being considered at a level that will lead to quantitative prediction of interfacial behavior.

In the past, the most attention has been paid to systems with fixed charge and with high-molecular-weight polymers (1–5). For example, with polyacrylamide–cationic random copolymers, the charge density along the backbone can potentially be controlled over a series of samples through the extent of quarternization or incorporation of quarternized cationic groups. For a substrate of fixed surface charge density, it is generally found that the surface coverage on the plateau of the isotherm increases sharply and then decreases gradually with an increasing degree of polycation quarternization (5). In the absence of chemical attractions between the polymer and the surface, a minimum amount of charge on the polymer is needed to overcome the entropic loss of adsorption. Greater amounts of charge on the polymer more effectively neutralize the surface charge so that with increased polymer quarternization, less polymer is needed to compensate the surface charge.

The situation is potentially more complex when both substrate ionization and polycation protonation are pH dependent (6–9). Not only will the bulk solution pH affect the coverage and interfacial configurations through variations in surface and polymer charge but also the local pH in the interphase, which depends on the local polymer density, will potentially further alter the polymer and surface charge. Hence there is an interplay between interfacial charge and polycation conformation. The influence of added salt further compounds the complexity, since salt will screen electrostatic repulsions between adsorbed chains (10, 11), but added ions can also compete with polymer segments for surface sites (4, 12). Additionally, in situations where the underlying polymer or surface charges are fairly concentrated, counterion condensation may limit the effective charge density (13, 14).

A number of fundamental questions therefore arise when trying to construct a complete picture of weak polycation adsorption.

1. How do pH and ionic strength affect the total adsorbed amount, interfacial configuration, and especially the amount of polymer bound to the surface locally in the form of trains?

[1] To whom correspondence should be addressed. E-mail: santore@mail.pse.umass.edu.

[2] Current address: Department of Polymer Science and Engineering, Conte Building, University of Massachusetts Amherst, Massachusetts 01003.

0021-9797/01 $35.00

2. Are the cation protonation and substrate ionization different in the interphase of an adsorbed layer compared with the bulk solution for a given pH and ionic strength?

3. Is there evidence that counterion condensation affects the binding strength, adsorbed amount, and interfacial conformations?

4. For situations where surface saturation corresponds to overcompensation of the underlying surface charge, what is the driving force for polycation adsorption beyond that needed to neutralize the surface charge?

The current paper is one of several publications addressing these issues, here focusing on the interfacial chain conformations in the context of surface and polycation charge variations. Detailed interpretations of interfacial ionization, counterion condensation, and differences between ionization at the interface and in the bulk are left to a second paper (15), due to space constraints.

In the current paper, NMR methods were utilized to measure coverage and interfacial conformation of a low-molecular-weight 15-unit dimethylaminoethyl methacrylate (DMAEMA) oligomer on colloidal silica, focusing on the effects of pH and ionic strength on the adsorbed conformation. It was anticipated that with the low-molecular-weight oligomer, adsorbed molecules would be mostly configured as trains, since the lack of chain length would prevent substantial formation of loops and tails in the context of classical homopolymer adsorption. Even so, variations in the number of electrostatic anchoring points on the surface and on the chain might cause subtle differences in these adsorbed oligomeric trains with pH and added salt. Hence, with an understanding of how the train conformation can vary, and with an understanding of how NMR can be employed to characterize the bound train fraction, it is then possible to move forward to probe the adsorbed configuration of higher molecular weight DMAEMA molecules where substantial loops and tails are possible. Therefore, the extension of the concepts developed in this work to polymeric DMAEMA is discussed in a third paper (16).

*Background on NMR*

In this paper, NMR methods were employed to probe two facets of polyelectrolyte adsorption: the isotherm for DMAEMA interactions with colloidal Ludox silica and the conformation of the adsorbed DMAEMA oligomers. To determine the isotherm, resonances for specific groups on the DMAEMA chain were examined. Additional information about the adsorbed DAMEMA conformation, especially the amount immobilized as trains (the part of the chain lying directly on the surface as opposed to extending from the surface in a tail or a loop), was deduced from the solvent relaxation behavior.

Adsorption isotherms were measured using liquid state proton NMR. Each datum on the isotherm employed a DMAEMA solution of known initial concentration. To this, a known amount of silica was added. The adsorbed amount was determined by comparing the peak areas of the resonance at a specific chemical shift before and after the addition of silica. Since adsorbed segments are relatively immobile and invisible in the NMR spectrum, the difference in the two peak areas directly gives the adsorbed amount. Further, the peak area after addition of colloidal silica yields the free solution calibration, plotted on the $x$ axis of the isotherm. Haggerty and Roberts employed this approach to characterize the adsorption of associative polymers (water-soluble polyethylene oxide chains with terminal alkane hydrophobes) on polystyrene latex and titanium dioxide particles (17). An analytical method that utilizes surfactant systems with and without polystyrene latex particles was employed to determine the capability of proton NMR to observe adsorbed surfactant close to the particle surface by means of detecting the oxyethylene resonance. Haggerty and Roberts were additionally able to characterize the extension of the PEO backbone away from the surface at increasing coverages, as a result of the increased mobility in PEO loops and/or tails.

While the polymer's chemical shifts contain primary information about adsorption, the same spectra also contain contributions from the solvent (99% $D_2O$), which provide further information about the conformation of adsorbed chains. Cosgrove *et al.* demonstrated the method of solvent relaxation and showed that for several nonionic polymers adsorbing onto silica, the train fraction was near unity at the lowest coverages (18–20). Then, with increasing coverage, loops and tails led to a reduction of the bound fraction.

In principle, NMR relaxation times are directly related to the molecular mobility. For small molecules such as solvents or low-molecular-weight species undergoing rapid motion, both the spin–lattice ($T_1$) and the spin–spin ($T_2$) relaxation times are inversely proportional to the correlation time (21). A $T_1$ value on the order of several seconds is common for water. When a given molecule is adsorbed at an interface, its molecular motion becomes constrained and relaxation becomes more efficient, so its relaxation times decrease by up to several orders of magnitude. The relaxation times of solvent molecules "bound" to an interface are similarly reduced by several orders of magnitude compared with the bulk solvent. As free solvent molecules exchange with those near a surface by means of either direct solvent exchange or spin exchange, the enhanced relaxation rate of the latter is propagated in an attenuated fashion through the entire solvent bath. Therefore, the enhancement of the observed solvent relaxation rate ($1/T_1$) is proportional to the amount of solvent constrained at the interface, that is, where the polymer trains sit on the surface. The NMR relaxation phenomena of aqueous silica suspensions have been investigated both theoretically and experimentally (22–25).

For solvent molecules which may reside in bulk solution or at an interface, the average relaxation rate is given by (18)

$$\frac{1}{T_1} \approx \frac{1 - P_i}{T_{1\mathrm{b}}} + \frac{P_i}{T_{1i}}, \qquad [1]$$

where $T_1$ is the observed relaxation time, $T_{1b}$ and $T_{1i}$ are the bulk and interfacial solvent relaxation times, respectively, and $P_i$ is the fraction of time each proton spends in the interface environment. Instead of relaxation time, it is covenient to use the specific relaxation rate $R_{sp}$,

$$R_{sp} = \frac{R_1}{R_1^o} - 1, \qquad [2]$$

where $R = 1/T_1$ for the solvent in the polymer/particle system and $R^o = 1/T_1$ of a reference silica/$D_2O$ solution without polymer. The use of 99% $D_2O$ significantly lengthens the $^1H$ $T_1$ of the residual protons in the solvent, increasing the sensitivity of the $R_{sp}$ measurement at 300 MHz.

Cosgrove *et al.* investigated the proportionality between $R_{sp}$ and the amount of adsorbed polymer as trains based on the equation, $A_{tr} = k^{-1} R_{sp}$, where $A_{tr}$ is the adsorbed amount of train segments and $k$ is the slope of the initial part of the curve of $R_{sp}$ *versus* the adsorbed amount (18). When $A_{tr}$ is divided by the corresponding total adsorbed amount, the train fraction can be obtained phenomenologically. They assumed a train fraction of unity at low coverage.

## MATERIALS AND METHODS

### *Oligomer*

Oligomeric DMAEMA was provided as a gift from Du Pont NEN (Wilmington, DE) and its structure is shown in Fig. 1. The 15-unit oligomer in the current investigation was synthesized by group transfer polymerization to yield chains with a molecular weight near 2350 and a relatively low polydispersity between 1.1 and 1.3 (26). As a result of the initiator, each oligomer contains a single methylmethacrylate monomer at one end of its chain. DMAEMA was provided in a polar organic solution of isopropanol and tetrahydrofuran. These low boiling solvents were replaced by dilution with $D_2O$, followed by solvent removal in a rotary evaporator for NMR studies. This process was repeated until no organic solvent peaks were apparent in the proton NMR spectrum. For experiments not requiring $D_2O$, a similar procedure was employed to replace the organic solvents with high purity deionized water (Milli-Q).

### *Silica Substrate*

A 12-nm-diameter Ludox colloidal silica suspension (Du Pont) with a surface area of 230 $m^2/g$ and 30% solid content by weight concentration was employed as the substrate. Samples of the silica suspension were purified using a 6000- to 8000-molecular-weight cut-off dialysis membrane or a 220-nm filtration membrane to remove ions and other contaminants. Though the pores in these filters exceeded the diameters of the colloidal particles, it was possible to conduct the dialysis or filtration for a finite amount of time, during which contaminants were removed (as gauged by conductivity) and an adequate concentration of silica particles was retained. After purification, NaCl was added back to the concentrated suspension at a concentration of $10^{-3}$ M to decrease the range of the repulsive interparticle potential, avoiding formation of a repulsive gel (27). Thus, the combination of purification and addition of ions resulted in samples whose ionic content was known exactly. In studies on the influence of salt, the colloids were used under conditions more dilute than this stock suspension, accessing NaCl concentrations as low as $10^{-5}$ M.

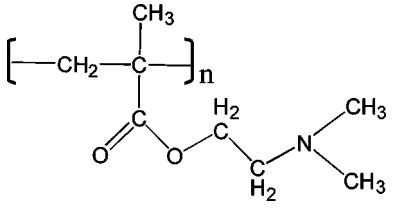


**FIG. 1.** Structure of the DMAEMA repeating unit.

### *Conductivity and pH Titrations*

Conductivity measurements were carried out using a Yellow Springs Instrument (YSI, Model 32) conductivity meter and a platinum immersion type electrode (YSI, Model 3403). pH titrations employed a conventional glass electrode with a Corning Model 30 pH meter calibrated by pH 4.00 and 7.00 standards (J. T. Baker).

### *Electrophoretic Mobility*

Electrophoretic mobility studies employed a DELSA 440 instrument manufactured by the Coulter Company (Hialeah, FL). A Coulter EMPSL7 mobility standard (0.04 g/L carboxylated polystyrene latex in 0.01 M sodium phosphate buffer, pH 7.0) was employed for calibration.

### *NMR Measurements*

All of the proton solution NMR experiments were performed on a GN-300 300-MHz FT-NMR spectrometer. A Nalorac 10-mm proton/broadband probe was utilized. Each sample was spun at 15–20 Hz. Samples were allowed to equilibrate at the desired temperature for a minimum of 10 min before the NMR experiment was performed. A 5-$\mu$s pulse width ($\sim 40^\circ$) was used. A 12-bit analog-to-digital converter was employed. The numbers of data acquisitions and data points utilized were 64 and 16,384 respectively. The acquisition time was 1.23 s with a dwell time of 150 $\mu$s. Butterworth audio filters matched to the dwell time increased the signal-to-noise ratio. Each signal-averaged free induction decay was multiplied by a decreasing exponential function equivalent to 0.8 Hz before one zero-fill and Fourier transformation. The relaxation delay time was set to 5 s to ensure quantitative NMR spectra.

All measurements were performed at room temperature, 298 K. To ensure accurate quantitative results, an external standard of tetrakis (trimethylsilyl) silane (TKS, Aldrich Chemical Company, Milwaukee, WI) was prepared in deuterated benzene

(99.9%, Cambridge Isotope Laboratories, Andover, MA) in a sealed glass insert tube. Chromium (III) acetonyl acetate was added to decrease the relaxation time of the external standard. In order to improve the dynamic range in this system, a presaturation solvent suppression method was applied (28), except for solvent relaxation experiments.

The inversion recovery experiment was performed to obtain the solvent $^1$H spin–lattice relaxation time, $T_1$, by detecting the amplitude of the free induction decay signal after the 90° pulse in an 180°-$\tau$-90° radiofrequency pulse sequence (29). In NMR studies, both DMAEMA and Ludox solutions were prepared from "neutral" $D_2O$ (Cambridge Isotope Laboratories). Dialysis was employed to remove small ions and measured the specific relaxation rate with respect to bare silica dispersions instead of deionized water. pD is reported rather than pH in this paper, except as noted. All NMR data were analyzed with NUTS1D software (ACORN NMR Co., Freemont, CA) after importing the FID data from the GN-300 NMR spectrometer.

## RESULTS

### *Protonation of DMAEMA*

In order to better understand the charge density of DMAEMA during adsorption, its solution behavior was first characterized using pH and conductometric titrations. The extent of protonation is shown in Fig. 2 for three different solution concentrations ranging from 1 to 50 eq/m$^3$. Prior to each titration with 0.1 M NaOH solution, each DMAEMA solution was treated with 0.1 M HCl to substantially protonate its tertiary amine groups. All the curves in Fig. 2 illustrate that at high pH (near pH 10), the DMAEMA is mostly uncharged; however, when the pH drops below 4.0, its amines are fully protonated. In the range of pH 8–9, DMAEMA is 10–20% protonated. The DMAEMA in the more concentrated solutions tends to be more protonated than in the more dilute solutions. This is expected, based on conventional electrolyte behavior: A weak polyelectrolyte will tend to dissociate more at lower concentrations.

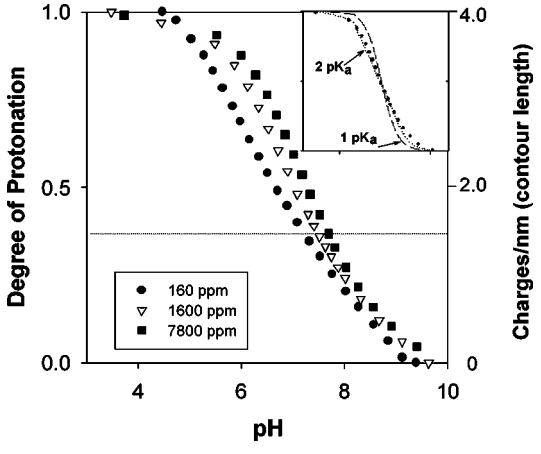


**FIG. 2.** Protonation curves from pH and conductometric titrations for three concentrations of DMAEMA: 7800 ppm (50 eq/m$^3$), 1600 ppm (10 eq/m$^3$), and 160 ppm (1 eq/m$^3$). Inset shows data for 7800 ppm, and best fits to one-p$K_a$ and two-p$K_a$ models. The dashed line presents the charge density at the Bjerrum length.

In Fig. 2, the right-most axis illustrates the density of protonated amine groups on the backbone, and provides a physical picture of the linear distance (down the backbone contour) between the positive charges on the backbone. This estimate of density of underlying positive charge on the DMAEMA backbone was determined by calculating the number of charges per 15-unit oligomer, and dividing by the contour length of 3.8 nm. While Fig. 2 summarizes the protonation behavior of DMAEMA based on pH and conductometric titrations, the protonation density down the backbone does not necessarily represent the actual charge density on the backbone, since counterion condensation will tend to reduce the actual positive charge.

Counterion or Manning's condensation (30–32) is expected to occur when the distance between two fundamental charges on the polymer backbone becomes so small that the work to bring them into proximity exceeds the thermal energy. This distance of approach, corresponding to 1 kT of energy, is termed the Bjerrum length and, for aqueous systems such as ours, is about 0.7 nm. It is defined as

$$\lambda_B = \frac{e^2}{4\pi\varepsilon_0\varepsilon kT}, \qquad [3]$$

where $e$ is the elementary charge, $4\pi\varepsilon_0\varepsilon$ is the dielectric constant of solvent, $k$ is the Boltzmann constant, and $T$ is the absolute temperature. Therefore in Fig. 2, while the right-most axis represents the underlying charge from protonated amine groups, the actual charge on the chain is expected to be capped at the Bjerrum length, indicated by the dotted line. Though the backbone may be more highly protonated at pH's below ~7.5, counterion condensation prevents the charge density from exceeding the Bjerrum length. An effective maximum protonation of about 35% is therefore estimated, occurring at pH 7.5 and below.

In the inset of Fig. 2, the individual titration curves are not adequately described by a single p$K_a$. A two-p$K_a$ model better approximates the data, capturing the possibility that after a first amine group is protonated, it becomes more difficult to protonate the amine of the neighboring monomer on a chain. Hence, alternate amine groups would tend to protonate first with one p$K_a$, while the amines between them would protonate at lower pH with the second p$K_a$. This two-p$K_a$ model is one of several possible explanations for the unusual titration behavior of this oligomer. A separate work addresses the protonation behavior of both the oligomeric and a high-molecular-weight DMAEMA, taking into account mobility changes from chain extension and counterion condensation (33).

Table 1 summarizes p$K_a$ values obtained by best fits to the titration curves for different polymer concentrations. The effect of added NaCl salt is also included in Table 1. While protonation is qualitatively similar at all salt concentrations, the p$K_a$ values are slightly increased at the highest salt concentration of

**TABLE 1**
**p$K_a$ Values of DMAEMA Solutions for Different Concentrations and Different Amounts of Added Salt**

| Concentration (ppm) | Two p$K_a$ model | | One p$K_a$ model |
|---|---|---|---|
| | p$K_{a1}$ | p$K_{a2}$ | Single p$K_a$ |
| 160 | 5.7 | 7.6 | 6.7 |
| 1600 | 6.3 | 8.0 | 7.0 (0 M, NaCl) |
| | | | 7.0 ($10^{-3}$ M) |
| | | | 7.1 ($10^{-2}$ M) |
| | | | 7.5 ($10^{-1}$ M) |
| 7800 | 6.4 | 8.0 | 7.3 |

0.10 M, suggesting that counterion condensation enhances the protonation of neighboring dimethyl amine groups. This observation is consistent with the findings of Hoogeveen *et al.* (1) who observed a similar effect with DMAEMA in 1 M NaCl.

*Ionization of Silica Particles*

Conductance and pH titrations on 0.4 wt% Ludox silica dispersions revealed the dissociation of the silica, summarized in Fig. 3. Prior to titration with 0.1 M NaOH solution, each sample was treated with 0.1 M HCl to substantially protonate its silanol groups. In Fig. 3, the surface becomes more negatively charged with increasing pH, with apparent p$K_a$ values near 9, though a single p$K_a$ value does not adequately describe any individual titration. p$K_a$ values in the range of 9.1–9.4 have been previously reported (34, 35) and are consistent with our findings. In Fig. 3, the magnitude of the surface charge density is on the order of 1 per nm$^2$ or less over the range of pH's employed in most of the adsorption studies (pH 9 and lower). At these relatively sparse surface charge densities, counterion condensation on the silica is not expected, since the fundamental charge spacing is greater than the Bjerrum length (0.7 nm).

Additional salt ions were found to increase silanol dissociation, also consistent with previous findings (4, 27). The point of zero charge, near pH 3.0–3.5 is also in agreement with the literature (36).

*Adsorption and the Influence of Ions*

In silica suspensions containing dissolved DMAEMA, the amine methyl proton NMR peaks of the DMAEMA were substantially reduced compared with the corresponding solution containing only DMAEMA and $D_2O$. This reduction in peak area facilitated calculation of the adsorbed amounts of DMAEMA on 12-nm Ludox silica in 99% $D_2O$. Ultimately for different DMAEMA concentrations and ionic strengths, adsorption isotherms were constructed. The adsorbed amounts found by this method were identical to coverages determined from examination of the resonances from the $-CH_2-$ and $-CH_3$ units of the main backbone. In these isotherm studies, the silica concentration was in the range of $0.4 \pm 0.002$ wt%.

In Fig. 4, coverages approaching 1 mg/m$^2$ were observed at high DMAEMA concentrations, on the apparent plateau of the isotherms. Added ions were generally found to increase the coverage, especially at the moderately concentrated and dilute regimes of the isotherms, below 4000 ppm. Added ions may promote adsorption by increasing the surface ionization (per Fig. 3) or screening lateral repulsions between adsorbed DMAEMA molecules. The latter may play some role in limiting the ultimate DMAEMA coverage on the pseudo-plateau.

In Fig. 4, the only ions added are from NaCl, which do not affect the solution pH significantly. As a result, the bulk solution pD increases with the amount of DMAEMA in the suspension, from about 8.5 in the dilute limit to a pD of 9.3 when the bulk solution concentration approaches 5000 ppm. Additionally, the protonation of the oligomer itself contributes to the ionic strength of the solution. For instance, at a bulk solution concentration of 4000 ppm, the free ions generated from protonation of both free and adsorbed polymer are on the order of $10^{-3}$ M. This latter

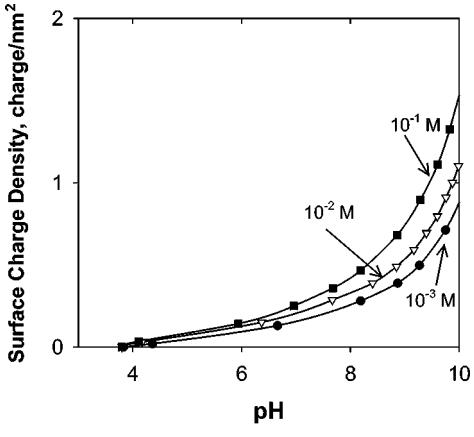


**FIG. 3.** Ludox 12-nm silica (0.4 wt%) ionization as a function of bulk solution pH, determined from pH and conductometric titrations, for different amounts of added salt.

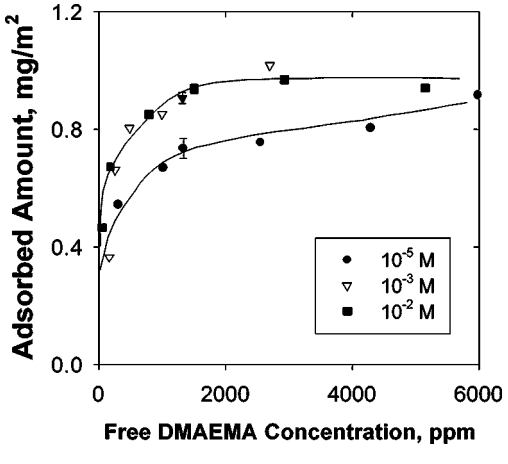


**FIG. 4.** Adsorption isotherms for DMAEMA oligomer on 12-nm Ludox in $D_2O$, for different amounts of added salt, determined by NMR measurements.

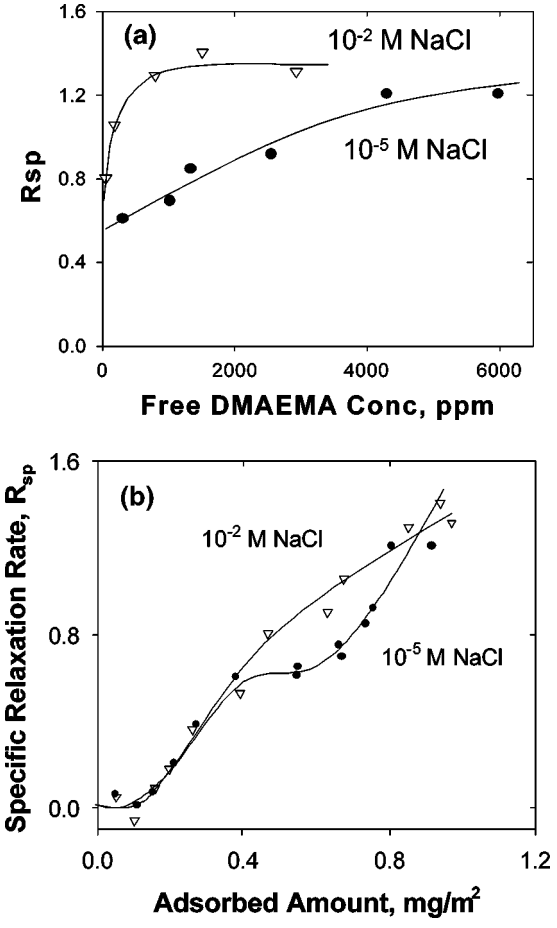


**FIG. 5.** (a) Solvent relaxation curves for the DMAEMA–Ludox suspensions in Fig. 4, shown in a form analogous to the adsorption isotherm, as a function of the remaining free DMAEMA concentration. (b) Solvent relaxation data for two ionic strengths, as a function of coverage. Data correspond to points on the isotherms in Fig. 4.

fact explains why the isotherms for the different nominal ionic strengths converge at high DMAEMA concentrations.

The observed influence of ions on the coverage in Fig. 4 and general speculations about the influence of ions on interfacial polymer chain conformations (37–40) motivated interpretation of the solvent relaxation in the context of the amount of trains. Figure 5a shows the solvent relaxation rate enhancement, $R_{sp}$, as a function of the free solution DMAEMA concentration (in the presence of Ludox silica), with data points corresponding to those of the isotherm in Fig. 4, for two concentrations of added NaCl ions, $10^{-5}$ and $10^{-2}$ M. As explained under *Background on NMR*, the quantity $R_{sp}$ is generally expected to be proportional to the mass of trains (segments) immobilized due to their adhesion to the surface. Therefore, from the general features of Fig. 5a and their similarity to the shapes of the isotherms in Fig. 4 (including larger $R_{sp}$ values for higher salt concentrations), one concludes that the amount of trains goes qualitatively as the adsorbed mass. There is more train mass on the plateau of the isotherm and more train mass for situations such as increased ionic strength which lead to more adsorbed DMAEMA. This is not a surprise because, with low-molecular-weight oligomers, chains are too short to form substantial loops and tails and the entire oligomer should lie close to the surface, if it adsorbs at all.

Since we are interested in the configurations of the adsorbed chains, specifically how much of the adsorbed mass is configured close to the surface as trains, we examined the dependence of $R_{sp}$ on the surface coverage in Fig. 5b. Data again correspond to points on the isotherm in Fig. 4 for two different amounts of added salt. At the lowest coverages, below 0.15 mg/m$^2$, $R_{sp}$ is independent of surface coverage and remains close to zero. Then, at coverages of 0.15 mg/m$^2$, $R_{sp}$ increases with adsorbed mass, suggesting that all adsorbing chains attain the same interfacial conformation or at least the same train fraction. This behavior continues for the full range of coverages at the modest NaCl concentration of 0.01 M; however, with the limit of extremely low ionic strength, the data start to flatten out before $R_{sp}$ increases again above surface coverages of 0.65 mg/m$^2$. Two features of Fig. 5b are unusual (but reproducible and easily resolved within the precision of the data) and warrant further examination: (1) the roughly zero slope of the $R_{sp}$ curve at low coverages below 0.15 mg/m$^2$, and (2) the plateau in $R_{sp}$ at intermediate coverages and low ionic strength.

The constant near-zero value of $R_{sp}$ at very low coverages was not observed in prior solvent relaxation studies of adsorbing nonionic polymers (polyethylene oxide (PEO) or polyvinyl pyrrolidone) (18), and appears to be a new feature found for this DMAEMA oligomer and also for higher molecular weight DMAEMA polymers (16). In the case of the previously studied nonionic polymers (18), $R_{sp}$ was linearly proportional to the train mass over the full range of coverages studied, with a $y$ intercept of zero in graphs analogous to Fig. 5b. In the case of DMAEMA, $R_{sp}$ increases with coverage only above 0.15 mg/m$^2$, even though one would expect these DMAEMA layers to consist mostly of trains, since the chains are too short to form substantial loops and tails.

Additionally, the low coverage limit, below 0.15 mg/m$^2$, corresponds to coverages where the Cosgrove lab found all-train configurations for PEO on silica. If one assumes that $R_{sp}$ is always proportional to train mass, then our data suggest no trains below 0.15 mg/m$^2$, which is an impossibility if adsorption occurs. Indeed, the lowest coverages provide the greatest opportunity for segment–surface interactions, which would give the highest train fraction. We must therefore interpret Fig. 5b to indicate that although $R_{sp}$ is insensitive to train mass below 0.15 mg/m$^2$, all chains adsorbed to the surface must be closely associated with it. The observation that $R_{sp}$ is unaffected at coverages up to 0.15 mg/m$^2$ suggests that at these low coverages the adsorbed trains are sufficiently mobile so that the solvent relaxation is not affected by adsorption.

At moderate ionic strengths corresponding to 0.01 M NaCl, the train fraction is roughly constant over the full range of coverages, decreasing slightly as the surface approaches saturation

above 0.7 mg/m$^2$. At the lower ionic strengths, for low coverages the same train fraction is observed up to 0.4 mg/m$^2$. Then as the adsorbed amount increases from 0.4 to 0.7 mg/m$^2$, there is very little increase in trains, suggesting that the average interfacial conformation is changing with coverage to include some segments that are loosely attached to the surface, as small tails or loops. This may result from repulsions within the adsorbed layer, which can be long range at the lowest ionic strengths.[3]

When more polymer is added to the system, giving higher coverages above 0.7 mg/m$^2$, the ionic strength is increased by ions brought along with the polymer. Indeed the overall ionic strength of the system with no added salt approaches that for the system to which salt was added, so one would also expect the adsorbed chain conformations to approach the same limiting behavior in the two cases. The increase in ionic strength resulting from the additional polymer in the system (needed to achieve coverages exceeding 0.7 mg/m$^2$) may screen long-range electrostatic repulsions, allowing chains to approach more closely or adsorb more flatly with decreased mobility.

*Influence of pH on Adsorption*

Figure 6a shows the coverages obtained at different pDs (since the solvent is deuterated water). pD was controlled with a 0.01 M buffer solution of NaOH and $KH_2PO_4$, giving overall ionic strengths (with buffering ions included, but not counting ions from the DMAEMA) varying from $1.2 \times 10^{-2}$ to $1.8 \times 10^{-2}$ M, depending on the solution. These ranges of ionic strength have minimal influence on coverages. In Fig. 6a, nominal pD values are indicated, corresponding to the dilute end of each isotherm. As a result of the basic nature of the DMAEMA the pD values increased roughly by 1/2 a pD unit as the free oligomer concentration was increased to about 2000 ppm.

At pH 6, the coverage was 0.4 mg/m$^2$, with a relatively flat isotherm plateau. At the higher pDs of 7 and 8, greater coverages were obtained and the plateaus of the isotherms were more gradual. At pD 12 (which was obtained using 0.1 M NaOH and $NaH_2PO_4$), however, the adsorption was negligible. This trend makes sense: At the lower pD's the oligomer has the greatest underlying charge, so that few chains are needed to saturate the surface, at least if the plateau corresponds to the charge compensation point. Also with more highly charged chains, there is a greater driving force for adsorption, leading to the flatter plateau. At higher pD values, the DMAEMA charge is decreased so that more oligomer is needed to compensate the surface charge. Finally, at the highest pD's, near 12, the DMAEMA is not charged at all, providing no driving force for adsorption. This lack of adsorption at high pD's also suggests that there is no chemical driving force for the adsorption of uncharged DMAEMA on silica.

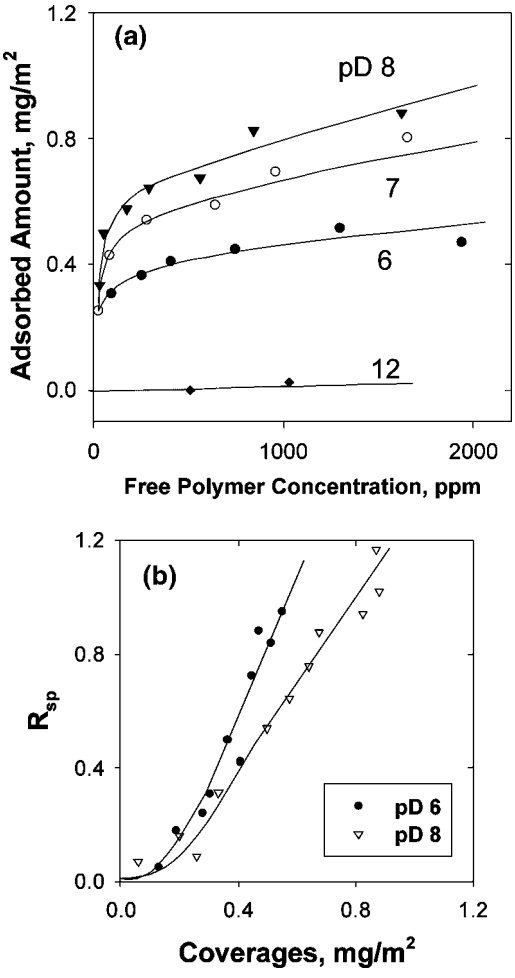


**FIG. 6.** (a) Adsorption isotherms for different pDs at moderate ionic strengths. (b) Solvent relaxation as a function of coverage for two of the isotherms in part (a).

Negligible adsorption was also observed at pH 1.8, maintained by HCl in $D_2O$. At these extremely low pH's, the DMAEMA is fully protonated; however, the silica bears a positive charge, which repels the oligomer.

Figure 6b shows the solvent relaxation rate enhancement as a function of coverage for two of the adsorption isotherms in Fig. 6a. (Data for the pD 7 isotherm are not shown simply to avoid crowding this figure.) Like Fig. 5b, $R_{sp}$ is independent of coverage below 0.15 mg/m$^2$. At higher coverages, $R_{sp}$ is linear in the adsorbed amount over the full range of coverages, with a greater proportionality constant at pD 6 compared with pD 8. This implies a greater train fraction for the adsorbed chains at pD 6 as opposed to pD 8. This observation is in qualitative agreement with expectations, since there is greater underlying charge on the polymer at pD 6 (70% protonation before counterion condensation) and less charge on the substrate. This would lead to flatter, less mobile chain conformations at pD 6 as opposed to pD 8. Though Fig. 6b does not illustrate $R_{sp}$ values at pD 12,

[3] An overall ionic strength of $0.5 \times 10^{-3}$ M is calculated for the dispersion containing $10^{-5}$ M NaCl and DMAEMA in sufficient amount to give 0.4 mg/m$^2$. Under these conditions, the Debye length is 2.8 nm while the distance between adsorbed oligomers is 1–2 nm. Thus there is substantial likelihood of inter-chain repulsion of adsorbed oligomers, causing reconfigurations and possibly small loops and tails with increased mobility.

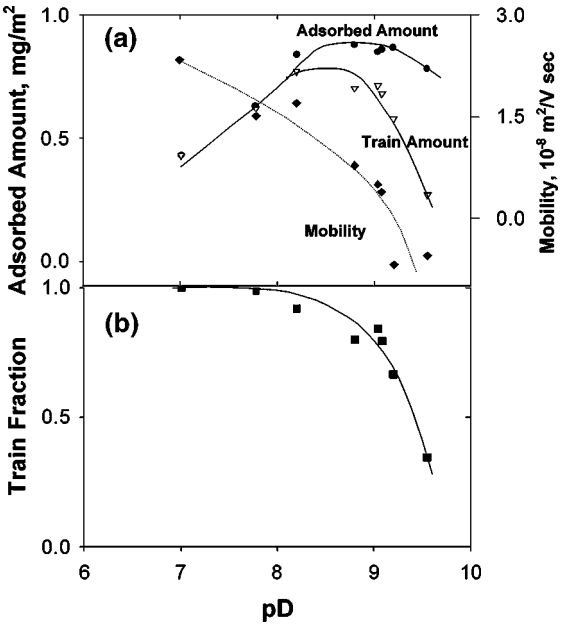


**FIG. 7.** (a) Adsorbed amount, train amount, and electrophoretic mobility for DMAEMA-containing dispersions on their respective isotherm plateaus. (b) Train fraction of adsorbed DMAEMA as a function of pD.

these were all nearly zero over the full range of DMAEMA concentrations considered, a result which is consistent with the observed lack of adsorption at pH 12.

Figure 7 shows the mobility, adsorbed amount, and train mass (fraction in Fig. 7b) roughly on the plateau of the isotherm for 0.01 M NaCl and different pD's. Of particular note in Fig. 7, the actual pD values have been measured, in contrast with the nominal pD values employed in the previous figure. These data correspond to a total DMAEMA concentration of 4000 ppm, which after adsorption onto 4.6 $m^2$ of silica gave remaining free concentrations of 3200–3600 ppm depending on the plateau coverages for particular adsorption conditions. In Fig. 7, the $R_{sp}$ values have been converted to train mass using two assumptions: (i) The train fraction for coverages below 0.15 mg/$m^2$ is the same as that for coverages just above 0.15 mg/$m^2$, within a data series at a particular pH and ionic strength. (ii) Of all the pD and ionic strength conditions tested, those exhibiting the highest slope on the $R_{sp}$ vs $\Gamma$ plot correspond to train fractions of unity. That is, at pD 7 and ionic strengths above 0.01 M, the DMAEMA adsorbs completely as trains. This second assumption is similar to assumptions made in prior works with PEO adsorption on silica.

In Fig. 7a in the pD range 7–10, the adsorbed amount goes through a maximum, as does the mass of adsorbed trains. The train fraction in Fig. 7b, however, decreases steadily as the pD rises above 7, while the train fraction is 1 at pD 7. At the low pD end of Fig. 7, all the adsorbed mass is in the form of trains, per assumption (2) stated previously, consistent with previous interpretations of $R_{sp}$ data. At the high pD end of Fig. 7, however, the train mass decreases more sharply with increased pD than does the total adsorbed mass. This suggests that as the DMAEMA protonation is decreased through increased solution pD, its binding to the surface is weakened, giving looser and potentially more mobile layers before the driving force for adsorption is completely lost at the highest pD's. At high pH, the DMAEMA protonation is decreased, so that there are fewer anchor points to the surface, allowing for the possibility of small loops or trains, or greater interfacial mobility.

The final data set in Fig. 7a, corresponding to electrophoretic mobility, shows a continued decrease in this property with increasing pD over the full range of pD values considered. Mobility is positive at all but the highest pD's, indicating a net-positive charge on the particles below pD 9. Since the data correspond to the pseudo-plateau of the isotherm where the surface is beginning to saturate with DMAEMA, one concludes that there is still a significant driving force for DMAEMA adsorption beyond the charge compensation point, that is, beyond the coverage where the surface charge is neutral on average. Interestingly, it is unlikely that there is a chemical driving force for the additional adsorption where the total particle charge is positive. This was shown by the lack of adsorption of nonprotonated DMAEMA, for instance, at pD 12. The potential driving forces for this surface charge overcompensation are explored more fully in a second paper (15). These include the possibility of increased surface silanol dissociation and increased DMAEMA protonation in the adsorbed layer compared with bulk solution, and the more likely explanation of patchwise adsorption, where surface regions containing adsorbed chains necessarily have a net positive charge, leaving some regions with residual negative charge. In the current paper, the observation of charge overcompensation is an interesting observation in the context of studying the interfacial chain conformation.

## DISCUSSION

In this work, the adsorbed conformation of a polycation oligomer was examined at a variety of pH's and ionic strengths, both as a fundamental exercise and as a basis for future quantitative interpretations of adsorbed high-molecular-weight cationic polyelectrolytes. For all conditions studied, data for coverages above 0.15 mg/$m^2$ were consistent with the previously established proportionality between the specific relaxation rate, $R_{sp}$, and the train mass. We have every reason to believe that the adsorbed conformations below 0.15 mg/$m^2$ are similar to those at moderately greater coverages, because at 0.15 mg/$m^2$, individual chains are isolated on the surface. At a coverage of 0.15 mg/$m^2$, there is 26 $nm^2$ of surface available, on average, to each chain. The individual chain contour length is 3.8 nm, which easily fits within this space. At a coverage of 0.15 mg/$m^2$, chains are also isolated from an electrostatic perspective. At the free polymer concentrations giving coverages near 0.15 mg/$m^2$, the maximum Debye length is 3 nm. Therefore the electrostatic repulsions between adsorbed chains at 0.15 mg/$m^2$ should be minimal. The insensitivity of $R_{sp}$ to adsorbed trains at coverages below

0.15 mg/m$^2$ therefore must be of different origin, still reflecting interfacial mobility.

It must be remembered that the $R_{sp}$ values measure interfacial dynamics as seen by the solvent molecules, with $R_{sp}$ values near zero suggesting that, from the perspective of the solvent, the adsorbed mass up to 0.15 mg/m$^2$ is in a very mobile state. This is the case for DMAEMA oligomers on silica (and high-molecular-weight DMAEMA polymers as will be shown in a future paper (16)), but not for polyethylene oxide adsorbed on silica (18), suggesting a fundamental difference in the adsorption of these two types of molecules. In the case of PEO, adsorption occurs by hydrogen bonding of the PEO's ether oxygens to nondissociated surface silanols. These ether oxygens are spaced roughly 0.4 nm apart on the PEO backbone, compared with an average spacing of 0.6 nm between nondissociated surface silanols at pH 7. In contrast, DMAEMA adsorption occurs primarily between protonated amines and ionized silanols, where the spacing of these two groups is shown as a function of pH in Figs. 2 and 3. If one considers a 2-nm section of PEO backbone (corresponding to the length of our DMAEMA oligomer), at pH 7 there is opportunity for as many as three to four segment–surface contacts involving the main PEO backbone. In contrast, for DMAEMA adsorption, for the range of pHs and ionic strength considered, only one to two segment–surface contacts per oligomer are expected. Furthermore, the DMAEMA interacts through the amine groups on its side chains, leaving the main backbone in a potentially more mobile state. The difference between adsorption by side chains of DMAEMA and main backbone of PEO is one factor which may contribute substantially to the difference in solvent relaxation, especially at low coverages. This may therefore explain why we see no effect of coverage on $R_{sp}$ below 0.15 mg/m$^2$ with DMAEMA, while the Cosgrove lab found $R_{sp}$ to be proportional to train mass over the full range of surface loading (18, 20).

With DMAEMA being anchored by only one to two points per oligomer, and with the amine anchoring points located on side chains rather than on the main backbone, it makes sense that adsorbed DMAEMA chains may appear more mobile to the solvent than adsorbed PEO on silica. One must then ask: Why, in the case of DMAEMA, does the mobility decrease, giving an increase in $R_{sp}$ at coverages of 0.15 mg/m$^2$ and above? It may be that though the surface is not yet crowded at 0.15 mg/m$^2$, the lateral mobility of the oligomers begins to be reduced due to the relatively lower availability of nearby open dissociated silanols on the surface. This remains one area of further exploration.

Despite the complexities arising from the mobile nature of adsorbed DMAEMA below coverages of 0.15 mg/m$^2$, when the ionic strength was moderate, the $R_{sp}$ values at higher coverages were linear in the adsorbed amount. This behavior was seen in $D_2O$ with added salt and at a variety of pD's maintained by buffer, and suggests that in layers of low or high coverage, the oligomers are roughly in the same average conformation. This is in contrast to the previously documented behavior of adsorbed PEO polymers (18), where at low coverages the changes in $R_{sp}$ with coverage were greatest, suggesting adsorbed trains. At higher PEO polymer coverages, $R_{sp}$ increased less with increasing interfacial mass, pointing to the development of loops and tails within the layer (18). In the case of DMAEMA oligomers, the chains are too short to form substantial loops or tails, which is why $R_{sp}$, and presumably the average adsorbed conformation, is relatively independent of coverage. It is interesting to note, however, that $R_{sp}$ does signal tighter binding at the lower pH's, where there is, on average, a slightly greater underlying charge per chain. This reduced mobility or relatively greater bound fraction at pH 6 was observed despite the potential for reduced backbone charge due to counterion condensation under these conditions.

## CONCLUSIONS

This work examined the adsorbed amounts and configurations of oligomeric DMAEMA on 12-nm colloidal silica particles, to gain perspective on the influence of ions and pH, and to lay the groundwork for probing adsorbed polymer conformations. The effect of pH was primarily to alter the surface density of potential adsorption sites, at the same time altering the underlying DMAEMA charge. The effect of pH on isotherm shape was consistent with the strongest binding near pH 6: Here the isotherm was flat and the coverage was the lowest, with the solvent relaxation indicating the least mobile interface of all the conditions considered. At higher pH's greater coverages were achieved, but the isotherms exhibited more gradual plateaus. Solvent relaxation was also suggestive of a more mobile interface, or a slightly smaller bound fraction. These observations were consistent with titration data indicating weaker charging of the DMAEMA with fewer attachment points per oligomer at higher pH's.

In the limit of the highest pH studied (at pH 12), the DMAEMA was unprotonated and no adsorption occurred, suggesting a purely electrostatic driving force for adsorption at the other pH conditions. As this limiting behavior was approached from the low pH side, the bound mass decreased more rapidly than the adsorbed amount, suggesting that the DMAEMA layers may contain small loops and tails or higher mobility, before adsorption disappears altogether.

At moderate ionic strengths at a particular pH, the bound train fraction was independent of coverage over the full range of coverages examined. This observation was contrary to prior findings with polymeric PEO adsorption on silica, where the bound fraction decreased with increasing coverage above 0.2 mg/m$^2$, suggesting the formation of loops and tails in the nonionic polymeric layer.

In the limit of low ionic strength, at low coverages oligomeric DMAEMA adsorbed with a relatively high bound or immobile fraction; however, at intermediate coverages near 0.4 mg/m$^2$, there was evidence of increased mobility, or at least the onset of small loops and tails, due to electrostatic crowding at the interface. As more oligomer was added to the system, however, the ionic strength was necessarily increased and the average

adsorbed conformation at the higher coverages (above 0.7 mg/$m^2$) was more similar to that at the lowest coverages.

This work also reported an interesting coverage dependence of $R_{sp}$ in the low coverage limit: For DMAEMA on silica below 0.15 mg/$m^2$, $R_{sp}$ was insensitive to coverage, suggesting an extremely mobile interphase even though the average bound fraction within each oligomer should have been similar to that at moderately higher coverages. This may be a result of the fundamentally different interfacial configuration of the adsorbed polycations, which adhere to the surface by relatively far-spaced amine side chains. This would leave substantial sections of the main backbone and nonprotonated side chains in a more mobile state from the perspective of the solvent.

## ACKNOWLEDGMENTS

This work was made possible by NSF support from Grants CTS-9817048 and EEC-9712915 and the Polymer Interfaces Center at Lehigh University. Many thanks go to M. Wolfe and H. Spinelli of Du Pont for their generous donation of the DMAEMA oligomer.

## REFERENCES

1. Hoogeveen, N. G., Cohen Stuart, M. A., and Fleer, G. J., *J. Colloid Interface Sci.* **182,** 133 (1996).
2. Sukhishvili, S. A., and Granick, S., *J. Chem. Phys.* **109,** 6861 (1998).
3. Lee, E. M., and Koopal, L. K., *J. Colloid Interface Sci.* **177,** 478 (1996).
4. Popping, B., Sebille, B., Deratani, A., Desbois, N., Lamarche, J. M., and Foissy, A., *Colloids Surf.* **64,** 125 (1992).
5. Bohmer, M. R., Heesterbeek, W. H. A., Deratani, A., and Renard E., *Colloids Surf. A* **99,** 53 (1995).
6. Cabot, B., Deratani, A., and Foissy, A., *Colloids Surf. A* **139,** 287 (1998).
7. Gebhardt, J. E., and Fuerstenau, D. W., *Colloids Surf.* **7,** 221 (1983).
8. Bonekamp, B. C., and Lyklema, J., *J. Colloid Interface Sci.* **113,** 67 (1986).
9. Sidorova, M., Golub, T., and Musabrekov, K., *Adv. Colloid Interface Sci.* **43,** 1 (1993).
10. Tanaka, H., Ödberg, L., Wägberg, L., and Lindström, T., *J. Colloid Interface Sci.* **134,** 219 (1990).
11. Williams, P. A., Harrop, R., Phillips, G. O., Pass, G., and Robb, I. D., *J. Chem. Soc. Faraday Trans. 1* **78,** 1733 (1982).
12. Durand, G., Lafuma, F., and Audebert, R., *Prog. Colloid Polym. Sci.* **266,** 278 (1988).
13. Manning, G. S., and Holtzer, A., *J. Phys. Chem.* **77,** 2206 (1973).
14. Satoh, M., and Komiyama, J., *Polym. J.* **19,** 1201 (1987).
15. Shin, Y., Roberts, J., and Santore, M., submitted (2001).
16. Shin, Y., Roberts, J., and Santore, M., submitted (2001).
17. Haggerty, J. F., IV, and Roberts, J. E., *J. Appl. Polym. Sci.* **58,** 271 (1995).
18. Cosgrove, T., Cohen Stuart, M. A., and van der Beek, G. P., *Langmuir* **7,** 327 (1991).
19. Cosgrove, T., and Griffiths, P. C., *Adv. Colloid Interface Sci.* **42,** 175 (1992).
20. Mears, S. J., Cosgrove, T., Thompson, L., and Howell, I., *Langmuir* **14,** 997 (1998).
21. Becker, E. D., "High Resolution NMR." Academic Press, New York, 1980.
22. Halle, B., *Mol. Phys.* **56,** 209 (1985).
23. Halle, B., and Piculell, L., *J. Chem. Soc. Faraday Trans. 1* **82,** 415 (1984).
24. Zimmerman, J. R., and Brittin, W. E., *J. Phys. Chem.* **61,** 1328 (1957).
25. Hanus, F., and Gillis, P., *J. Magn. Reson.* **59,** 437 (1984).
26. Sogah, D. Y., Hertler, W. R., Webster, O. W., and Cohen, G. M., *Macromolecules* **20,** 1473 (1987).
27. Iler, R., "The Chemistry of Silica." Wiley, New York, 1979.
28. Martin, M. L., Delpuech, J.-J., and Martin, G. J., "Practical NMR Spectroscopy." Heyden, London, 1980.
29. Kingsley, P. B., *Concepts Magn. Reson.* **11,** 243 (1996).
30. Manning, G. S., *J. Chem. Phys.* **51,** 924 (1969).
31. Manning, G. S., *J. Chem. Phys.* **51,** 934 (1969).
32. Danutzenberg, H., Jaeger, W., Kotz, J., Phillipp, B., Seidel, Ch., and Stscherbina, D., "Polyelectrolytes." Hanser, New York, 1994.
33. Shin, Y., Ph.D. thesis, Lehigh University, Bethlehem, PA, 2002.
34. Kokufuta, E., Jujii, S., Hirai, Y., and Nakamura, I., *Polymer* **23,** 452 (1982).
35. Perrin, D. D., "Ionization Constants of Inorganic Acids and Bases in Aqueous Solution." Pergamon, New York, 1982.
36. Ross, S., and Morrison, I. D., "Colloidal Systems and Interfaces." Wiley, New York, 1988.
37. Bohmer, M. R., Evers, O. A., and Scheutjens, J. M. H. M., *Macromolecules* **23,** 2288 (1998).
38. van de Steeg, H. G. M., Cohen Stuart, M. A., de Keizer, A., and Bijstebosch, B. H., *Langmuir* **8,** 2538 (1992).
39. Sudholter, E. J. R., and Engberts, J. B. N., *J. Phys. Chem.* **83,** 1854 (1979).
40. Fleer, G. J., Cohen Stuart, M. A., Scheutijens, J. M. H. M., Cosgrove, T., and Vincent, B., "Polymers at Interfaces." Chapman & Hall, London/New York, 1993.